COBEM-2017-0390
PRODUCTION OF ALN THIN FILMS VIA DEEP OSCILLATION MAGNETRON SPUTTERING FOR BIOSENSORS

Olimpia Salas
Tecnológico de Monterrey-CEM, Carretera al Lago de Guadalupe km 3.5, Atizapán de Zaragoza, México, 52926 México
osalas@itesm.mx

Jianliang Lin
Southwest Research Institute, San Antonio TX, 78228-0510 USA
jianliang.lin@swri.org

Lizbeth Melo-Máximo
Tecnológico de Monterrey-CEM, Carretera al Lago de Guadalupe km 3.5, Atizapán de Zaragoza, México, 52926 México
nimbus3600@hotmail.com

Abril E. Murillo
Tecnológico de Monterrey-CEM, Carretera al Lago de Guadalupe km 3.5, Atizapán de Zaragoza, México, 52926 México
erendiramurillop.31@gmail.com

Dulce Melo-Máximo
Tecnológico de Monterrey-CEM, Carretera al Lago de Guadalupe km 3.5, Atizapán de Zaragoza, México, 52926 México
virimelo@itesm.mx

Jacqueline Oliva-Ramírez
Tecnológico de Monterrey-CEM, Carretera al Lago de Guadalupe km 3.5, Atizapán de Zaragoza, México, 52926 México
liszetholiva@gmail.com

Abstract. *Al/AlN thin films were produced by Deep Oscillation Magnetron Sputtering (DOMS) on two different substrates: 304L stainless steel and Si wafer. The structural differences between the resulting films were analyzed and compared as well as their response to biofunctionalization. The films were characterized by glancing angle x-ray diffraction, scanning electron microscopy + energy dispersive analysis, optical profilometry, and atomic force microscopy. The results indicate that the quality of the films for their use in biosensors was excellent. The films had a dense columnar structure, with low roughness, and exhibited a strong (002) preferential orientation. The material of the substrate did not exert a great influence on the texture and columnar film morphology of the AlN films. However, the substrate material did affect the nucleation step of film formation and this resulted in differences in density, surface roughness and extent of compressive residual stresses in the films. Thus, the nature of the substrate can be used to help tailor these film features. Biofunctionalization of the top AlN layer surface was successfully carried out and seemed to be affected by the surface characteristics of the AlN. However, further optimization of the biofunctionalization method is required to obtain more information.*

Keywords: *AlN thin films, acoustic biosensors, deep oscillation magnetron sputtering*

1. INTRODUCTION

The use of sputtering deposition techniques in the development of biosensors has attracted great attention in the past few years. The reasons behind this interest lie primarily in the ability of these techniques to produce high quality thin films at low temperature and their relatively easy insertion into microfabrication processes. In particular, the production of acoustic biosensors, requires the deposition of a piezoelectric thin film, often AlN or ZnO, with specific features. The central film characteristic sought is preferential orientation of the films along <001> for the best piezoelectric response is observed along this direction. Other important features include good density, low surface roughness, controlled residual stresses, and good adhesion. For the case of AlN thin films, there are many studies regarding deposition by magnetron sputtering, either with direct current (d.c.) (Iqbal A. *et al*, 2016 and Ait Aissa K. *et al*., 2015) or radio-frequency (r.f.) (Clement M. et al., 2003 and Caliendo C. *et al*., 2003) to cite a few. However, the use of the most recent high power impulse magnetron sputtering (HIPIMS) techniques for this particular application has been barely explored (Ait Aissa K. *et al*., 2015). In these deposition methods, high power pulses are applied to the target for very short periods. As a result, plasmas with high ion density are produced without excessive heating of the target. Applying a negative bias voltage to the substrate allows for the control of bombardment energy of the ion flux to tailor the features of the films (Gudmundsson J.T. *et al*., 2012). However, one of the drawbacks of HIPIMS is the generation of arcs due to the unipolar nature of the associated target voltage pulses. To alleviate this problem, in the DOMS technique, long voltage pulses composed of smaller oscillating pulses are applied, and an almost arc-free deposition can be carried out under adequate processing parameters (Lin J., *et al*., 2013). A schematic comparison of the waveforms in

HIPIMS and DOMS is presented in Figure 1. In addition to the possibility of arc-free operation, the application of high voltage pulses to the target in DOMS, also results in high ionization of the sputtered material. This highly ionized plasma has the potential to produce films with good crystallinity, fine columns, preferred orientation, and high density, even without the use of substrate bias voltage or external heating. Behind these enhanced features, is the abundant bombardment of the film with sputtered ion species in addition to electrons and gas ions, not available in conventional magnetron sputtering techniques. This bombardment leads to the high adatom mobility required to produce such structural features. However, careful control of the deposition conditions is needed to avoid excessive ion bombardment that may lead to high residual stresses or generation of crystal defects in the films (Oliveira J.C. *et al*. 2015, and Lin J. *et al*., 2017)

In the present work, the potential to produce Al/AlN films for acoustic biosensors by DOMS has been explored. The films were deposited on two substrate materials, Si (100) wafer and 304L stainless steel, and the structural features relevant for its use as piezoelectric thin films for acoustic biosensors extensively characterized.

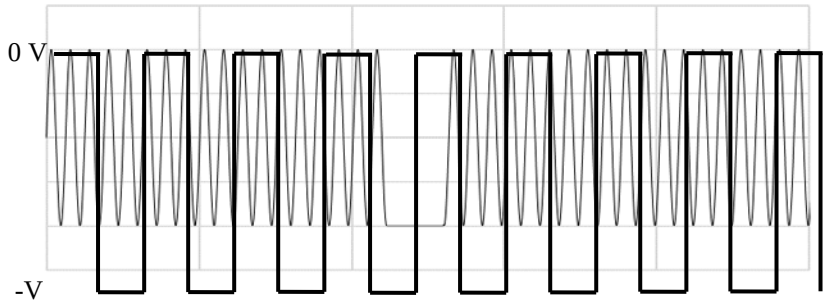

Figure 1. Schematic waveforms for HIPIMS (bold line) and DOMS (single line)

2. EXPERIMENTAL PROCEDURE

2.1 Deposition experiments

The deposition experiments were carried out in an unbalanced magnetron sputtering system (CFUBMS). A magnetron with a high purity (99.9%) Al target was used for the depositions. Substrates (Si (100) wafer and 304L stainless steel) were mounted on a holder 80 mm away from the target. Substrates were cleaned and then an Al adhesion layer was deposited. For both, the Al and the AlN depositions, the Al target was powered by deep oscillation magnetron sputtering (DOMS) (Zond, Inc.) at a constant average power of 1.0 kW. The peak voltage and peak current during the pulses were 515 V and 64 A, respectively. The pulsing frequency and duty cycle were 812 Hz and 78%. In the case of the AlN deposition, the Ar and N_2 flow rates were maintained at 50 sccm and 21 sccm, respectively, to maintain a constant working pressure of 0.67 Pa. A substrate bias voltage of -40V was applied for the depositions. The total deposition time was 120 min. Further details can be found in (Lin J. *et al*., 2017).

2.2 Characterization of films

Characterization of the films was carried out by several techniques. Scanning Electron Microscopy (SEM) was performed in a Jeol 6360LV microscope equipped with Energy Dispersive Spectroscopy (EDS). Glancing Angle X-ray Diffraction (GAXRD) was conducted at 40 kV and 25 mA with Cu-Kα radiation in a Bruker D8 ECO-ADVANCE apparatus. Atomic Force Microscopy (AFM) was performed in a Bruker BioScope Catalyst apparatus.

2.3 Biofunctionalization experiments

In order to immobilize the antibodies anti-HER2 protein, the protein G was first coupled (invitrogenXX) with an overnight incubation in phosphate saline buffer at 4°C. The films were washed with TBS-Tween and blocked with PBS-10% bovine serum albumin for 30 minutes at 37°C. To remove the remaining albumin, the films were washed again with TBS-Tween and rinsed with PBS to take out the tween residues. Anti-HER2 antibody (HER2 (c-erbB-2) Mouse Monclonal Antibody (clone TAB250), Concentrate #280003Z) was incubated 1.5 h at room temperature, followed by rinsing with TBS-Tween and PBS. Blocking and cleasing were carried out as above. HuHER2 protein was reconstituted with 1mL of standard diluent buffer (human HER2 Total #KHO0701; Invitrogen Corporation, Carlsbad, CA, USA) and incubated in the films (12.5ng/mL) for 2 hour at room temperature. After incubation, the supernatant was discarded and washed with the kit wash buffer (10 mM phosphate buffer [pH 7.4], 150 mM NaCl, 0.05% Tween 20) to remove the unbound protein. Detection antibody was added and incubated for 1 h at room temperature. To reveal the antibody-antigen complex it was labeled with secondary antibody anti-IgG FITC conjugated, incubated for 30 min at room temperature, washed with PBS and fixed with 4% of formaldehyde. The images were obtained by fluorescence

microscope (Olympus, BX51), the data analysis was performed with Image J 1.51m9 (Wayne Rasband, NIH, USA) and GraphPad Prism5.

3. RESULTS AND DISCUSSION

3.1 Microstructural Characterization

SE (secondary electron) images of the two samples in figure 2 show the morphological features of the films. In both cases, the surface was smooth and correspondingly, the cross-sectional views reveal a fine, dense columnar structure. The columnar growth was straight and perpendicular to the substrate surface. The thickness of the films were approximately 1.76 μm and 1.7 μm for the films deposited on the Si and 304L substrates, respectively. The deposition conditions, including the deposition time, were the same for both films, thus it can be inferred that the AlN formed on the Al/304L substrate was a bit denser.

The composition of the films was evaluated by EDS, and the results are presented in figure 3 below. The peaks corresponding to the films were only from Al and N, and a little signal form the substrates was also present. X-ray photoelectron analysis (not included here) of samples obtained in similar conditions revealed an almost 1:1 Al/N ratio, this is a very close to stoichiometric AlN films.

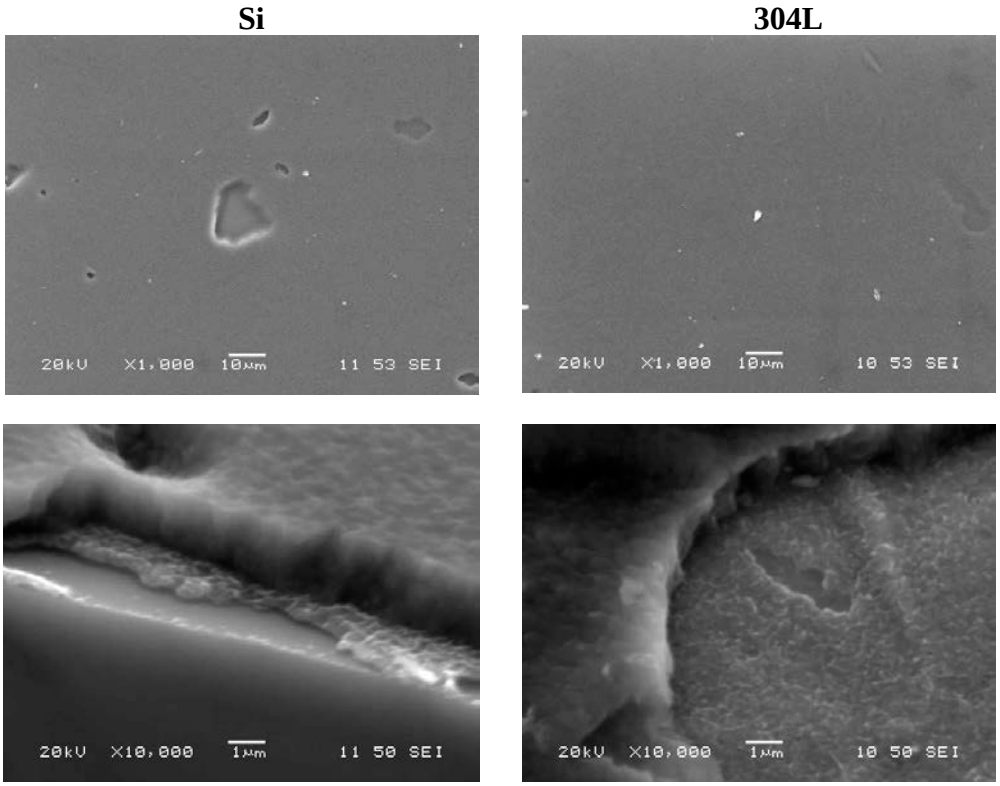

Figure 2. SEM views of the Al/AlN films on the Si and 304L substrates.

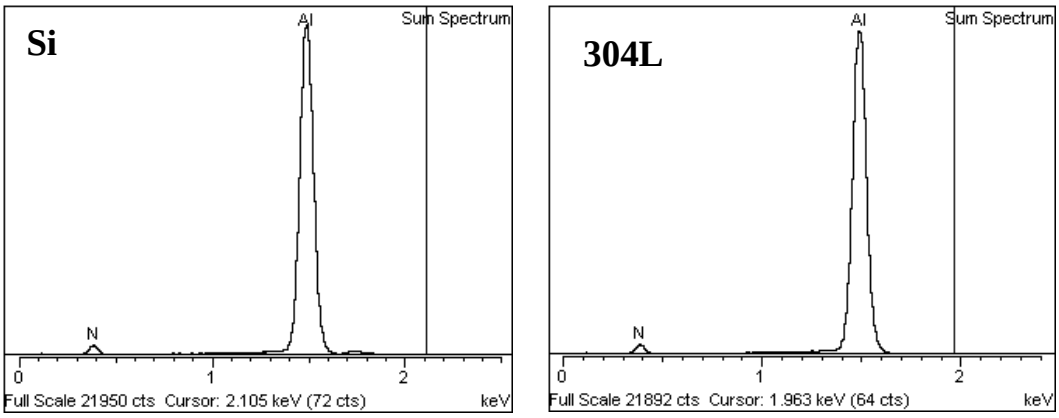

Figure 3. EDS spectra from the Al/AlN films on the Si and 304L substrates.

The surface roughness of the samples was evaluated both by AFM. The results, in figure 4, indicate that the AlN deposited on the 304L substrate had slightly lower roughness. The values in this table are similar to the higher values obtained by Yang Y-C (Yang Y-C. *et al.*, 2014) and higher than those by Chang C-T et al. (Chang C-T. et al., 2014), both for AlN films deposited by HIPIMS. These results are discussed below.

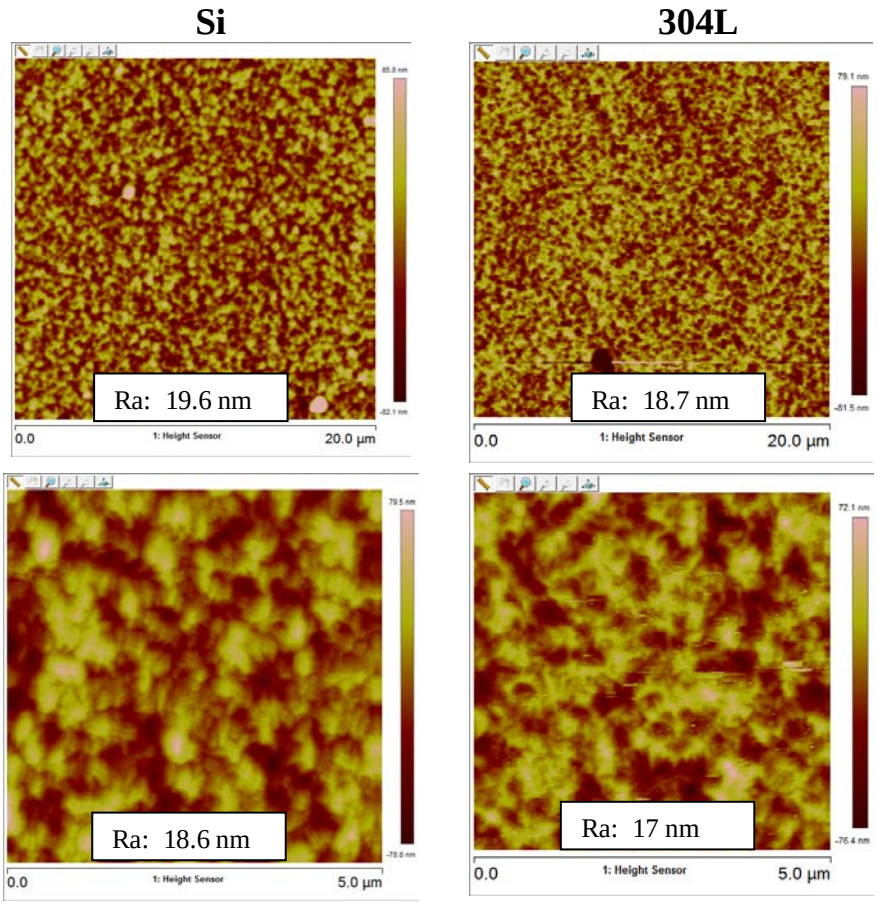

Figure 4. AFM images form the surface of the Al/AlN films deposited on Si and 304L. The top and bottom row correspond to a 20µm X 20µm and 5µm X 5µm scanned areas, respectively.

Phase identification was carried out by GAXRD and the results are included in figure 5. These images show that the AlN films had a clear (002) preferential orientation, regardless of the substrate material, indicating that the adatoms at the surface had enough mobility to produce the lowest energy (002) planes in both cases. There were however some differences in the GAXRD results. In the AlN film deposited on the 304L substrate, the (002) peak was much more intense than that on the Si substrate, even though the thickness of the AlN film on the 304L substrate was smaller. As mentioned above, one possibility is that the AlN film formed on the 304L substrate was denser than that on the Si substrate. Also, in both diffractograms the position of the h-AlN (002) peak was to the left of that for the bulk unstrained value (JCPDS 21-1133), and even more to the left for the film on 304L substrate. This indicates the presence compressive residual stresses in the films, and a higher level for the film on the 304L sample. This is not surprising, as a relatively high negative bias voltage was applied on the substrates. Finally, it is interesting to note that despite the similar thicknesses of the AlN films, the Al reflections corresponding to the bond layer were only present in the diffractogram of the 304L sample. It suggests that the Al layer on the Si substrate may have been thinner and/or have a certain degree of amorphous structure.

Thus, although in both cases a (002) AlN film texture was obtained, it seems that the substrate had an effect on several features of the Al/AlN films. Since deposition on both substrates was carried out in the same conditions, the differences should be attributed to the substrate material. Features of the substrate that may have influenced the final AlN film structural features, include its crystal structure, thermal expansion coefficient and its effect on the structure of the adhesion layer. Regarding the later, García-Farrera et al. (García-Farrera *et al.*, 2016) observed that the features of an Al adhesion layer affected the phase selection and thickness of AlN films deposited by radio frequency magnetron sputtering. On the other hand, the differences in residual stresses may be related both to stresses associated to film growth, but also to differences in thermal expansion coefficients during heating and cooling of the samples.

The effect of the substrate on the Al adhesion layer and this in turn on the characteristics of the AlN films has to consider the various processes involved in the formation of thin films. These include adsorption (physical or chemical),

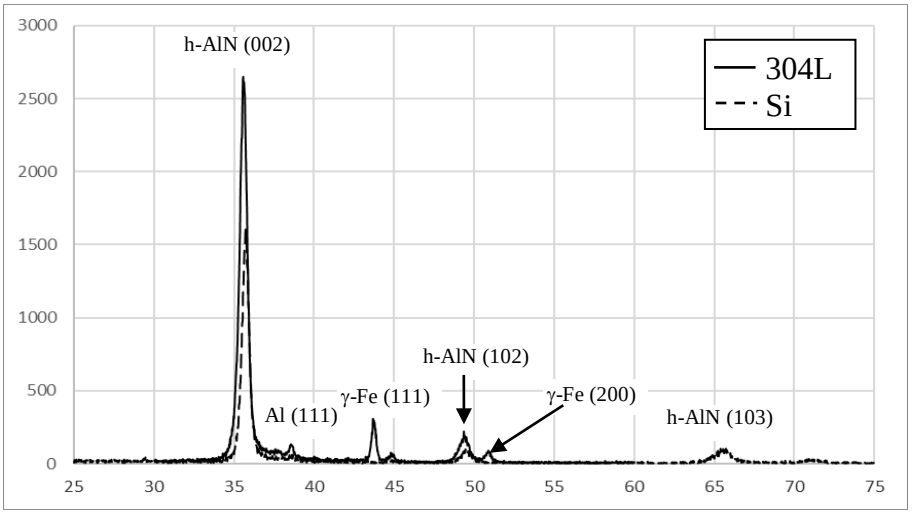

Figure 5. GAXRD patterns from the surface of the Al/AlN films on Si and on 304L.

diffusion, reaction of the arriving species, and then nucleation and growth of the film. Of the first three, adsorption and reaction are more likely to be affected by the substrate material, particularly by the chemical affinity between the substrate Fe atoms and the incoming Al species. In this regard, the affinity of Al for ferrous materials is expected to be stronger than for Si. As a result, the sticking coefficient on the 304L should be larger than on Si, which is important for nucleation. The temperature reached in both substrates was similar, as well as the energy with which the species arrived on the surface, thus diffusion, i.e. atom mobility should have been similar on both substrates. In particular, due to the substrate temperature reached (slightly higher than 0.3Tm in either substrate) and the high energy of the incoming species, high ad-atom surface mobility was not limited. The next step, nucleation, is also affected by the affinity between species as well as by the density nucleation sites. From the three modes of nucleation: 2-D or Fran der Mower, 3-D or Velmer-Weber, and Strarski-Krasnopov (S-K), it would be expected that given the larger affinity of Al for Fe than for Si, nucleation of Al on Fe be closer to S-K and to 3-D on Si. In any case, although a certain degree of surface roughness will result from these types of nucleation, a tendency to small nuclei size is resulted from breaking of the formed nuclei by the energetic incoming species. However, since the surface of the 304L steel was polycrystalline and likely to have more irregularities than the Si (001) flat wafer, it must have favored a more copious nucleation, which led to finer nuclei when they coalesce. After nuclei coalescence, there follows growth. In the present conditions, in which the homologous temperature is above 0.3 in both cases, growth is expected to follow the Thornton Zone T mode (Anders, 2010). Additionally, if the effect of the high energy of the incoming particles and typical energy distributions for metal ions in DOMS (Ferreira *et al*., 2017) are considered, the model developed by Anders (Anders, 2010), indicates that compressive stresses and preferential orientation are possible within the conditions of the present study. In terms of the Al bond layer, it is difficult to assess level or type of residual stresses and preferential orientation as the layer is underneath the top AlN.

In summary, a finer, denser and smoother columnar structure of the Al bond layer formed on the 304L substrate, while on the Si surface, the Al columns were slightly larger and less dense. The main reason behind this structure was the easiness of copious heterogeneous nucleation on the 304L surface, followed by Zone T fine columnar growth, both aided by enhanced adatom mobility from the accelerated particles and ions towards the surface of the growing film. The formation of the AlN films was influenced by the structural characteristics of the Al bond layers. In both cases, the nucleation of AlN on the Al surface was likely to have been the 3-D type of nucleation, as the affinity for Al ions for N ions is very high, although some of the Al and N ions must have also reacted with the surface Al atoms. In both cases, breaking-up of nuclei due to ion bombardment occurred and led to fine structures. As a result a fine surface roughness was obtained on both substrates. However, the finer roughness of the Al on 304L provided more nucleation sites, thus a finer, denser nucleation of the AlN must have occurred on top of this sample. For the growth of the AlN, the higher melting point of this material results in a homologous temperature of around 0.24, which without energetic ion bombarding, would result in Zone 1 type of growth. However, it is clear from the cross-sectional views that the columnar growth of the AlN was also in the Zone T-Zone 2 regime of tight columns due to ion bombardment. Furthermore, the higher nucleation rate on the 304L produced even tighter columns, this is a finer, denser AlN structure, which explains the higher (002) peak in the GAXRD graph of this sample.

Regarding the level of residual compressive stresses in the samples, there are two possible sources for the higher value observed for the sample on the 304L substrate. One is the expected higher tensile growth stress in the Si sample due to more open columnar structure and the other is the different levels of thermal induced stresses during cooling. The coefficients of thermal expansion for Si, 304L, Al, and AlN are 3-5, 17.3, 21-24, and 5.3 10^{-6} K^{-1} (TET, 2017),

respectively. Thus, the lower coefficient for the Si substrate produced tensile stresses in the Al/AlN film architecture, mainly through the Al layer that is next to the substrate and has a much larger difference in thermal expansion coefficient with Si. Both tensile stresses counteracted to some extent the compressive stresses produced by ion bombarding, but did not eliminate them completely. Thus, residual stress can be controlled to a certain extent through the nature of the adhesion layer.

3.2 Biofunctionalization experiments

Figure 6 shows the images from fluorescence microscopy from a non-biofunctionalized (control) and a biofunctionalized region from the surface of both samples (304L and Si). Although the images are dark, there is a clear fluorescence signal on the biofunctionalized areas of both samples (see circles), while the control samples are uniformly dark. Considering the weak signal observed in figure 6, probably due to less sensibility of the secondary antibody anti-IgG FITC, further analysis of these images was carried out with an image analyzer (Image J software). The results are shown in figure 7 as the median fluorescence intensity (MFI), which provides more information than the images. The analysis also indicated that the surface had self-fluorescence, thus a basal MFI can be seen on this graph from the control areas. Both figures show that the AlN film was able to be biofunctionalized. However, we must consider further analysis to find a method to overexpress the signal. These results also show that the surface characteristics of the Si sample had a slightly higher biofunctionalization response.

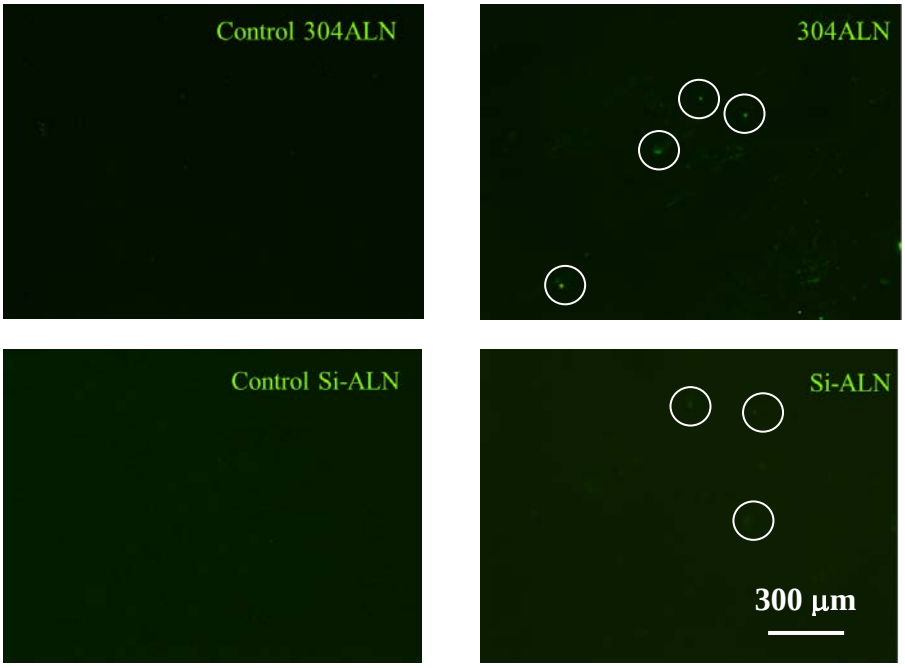

Figure 6. Fluorescence microscopy images from non-biofunctionalized (control) and biofunctionalized areas on the surfaces of both samples.

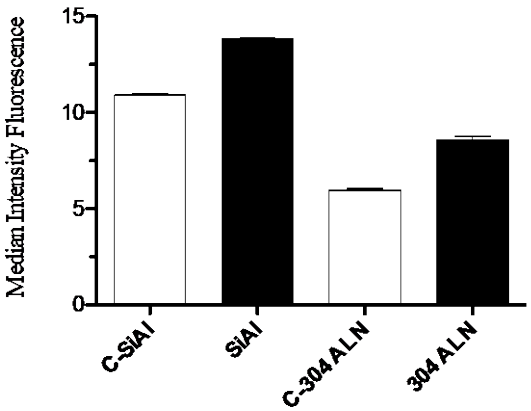

Figure 7. Median Fluorescence Intensity from the surface of the non-biofunctionalized (control) and biofunctionalized areas on the surfaces of both samples.

Additional analysis of the non-biofunctionalized and biofunctionalized surfaces was carried out by SEM+EDS. Figure 8, shows the SE images and corresponding EDS analyses for both samples. In the case of the non-functionalized surfaces, only the morphology of the top AlN film was observed. However, in the case of the biofunctionalized areas, there formed a discontinuous network of particles on the surface of the AlN. It is not possible at this point to relate this structure to the actual attachment of the antibodies, however it is clear that the surface in the biofunctionalized regions underwent a morphological change. Furthermore, the EDS analysis of these regions showed the presence of C and O, which points to its biological nature, while the non-biofunctionalized Al surface only displays the signal from Al and N corresponding to the AlN/Al film. These images, however, did not provide enough information to discern the origin of the slightly better response of the Si sample to biofunctionalization observed in figure 7.

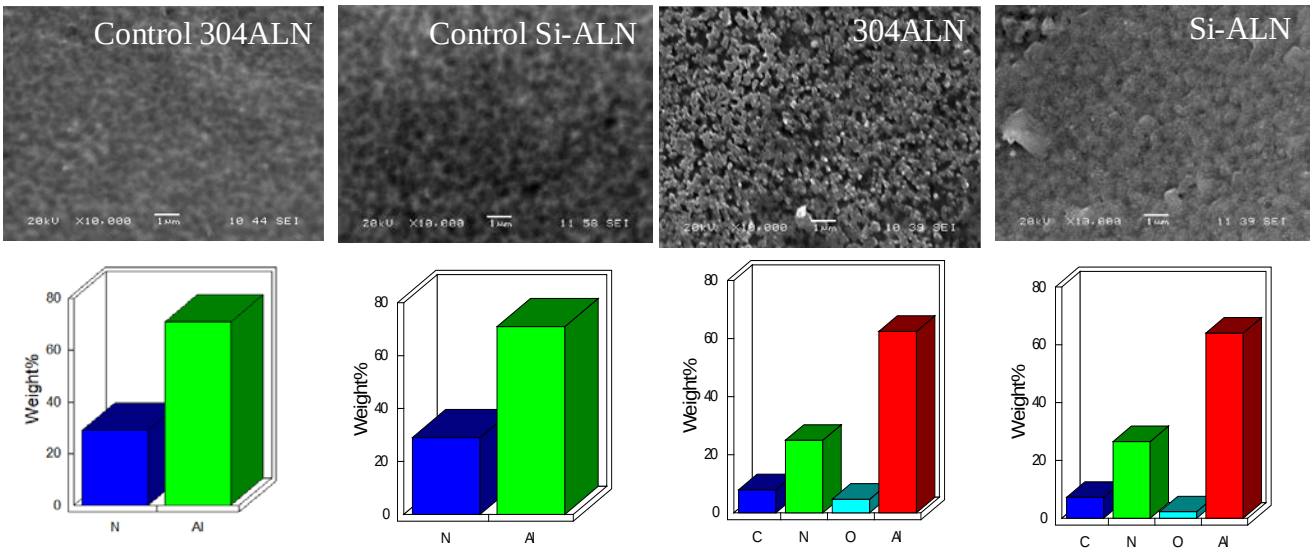

4. CONCLUSIONS

Highly c-axis oriented columnar AlN thin films were produced on Si (100) and 304L substrates by DOMS without any external heating. The substrate material did not affect the texture nor columnar morphology of the films. However, other film features indicated that the substrate material may have affected the nucleation of the Al bond layer on the substrate and this in turn affected the density, surface roughness and residual stresses in the films. The higher affinity of Al for Fe than for Si, as well as the higher nucleation sites on the rougher 304L surface, resulted in a finer, denser columnar morphology of the AlN films on this substrate. Compressive residual stresses were observed in both films, mainly as a result of the energetic ion bombardment due to the negative applied voltage. However, these were lower in the film on Si (100) likely due to the more open columnar structure and larger difference in thermal coefficient expansion. The present results then indicate that some film features can be controlled to some extent through the nature of the substrate material. The biofunctionalization experiments showed that attachment of biomarkers can occur on the surface of the AlN films, however refinement of the biofunctionalization method is required to provide better results. There seems to be an effect of the surface characteristics of the AlN film on the biofunctionalization response that has to be further investigated.

5. ACKNOWLEDGEMENTS

We want to thank and acknowledge the assistance provided in the following laboratories in México to perform the GAXRD and AFM experiments: *Termoinnova, S.A. de C.V.*, and *Centro de Nanociencias*, IPN, México, respectively. Part of the biofunctionalization experiments was carried out at the laboratory of *Inmunología Celular*, Cinvestav, IPN, México.

6. REFERENCES

Aissa, A. K., Achour, A., Elmazria, O., Elhosnni, M., Boulet, P., Robert, S. and Djouadi, M.A., 2015. "AlN films deposited by dc magnetron sputtering and high power impulse magnetron sputtering for SAW applications". *Journal of Physics D: Applied Physics*, Vol. 48, p. 145307.

Anders, A., 2010. "A structure zone diagram including plasma-based deposition and ion etching". *Thin Solid Films*, Vol. 518, p. 4087.

Caliendo, C., Imperatori, P. and Cianci, E., 2003. "Structural, morphological and acoustic properties of AlN thick films sputtered on Si(001) and Si(111) at low temperature". *Thin Solid Films*, Vol. 441, p.32.

Chang, C-T., Yang, Y-C., Lee, J-W. and Lou, B-S., 2014. "The influence of deposition parameters on the structure and properties of aluminum nitride coatings deposited by high power impulse magnetron sputtering". *Thin Solid Films*, Vol. 572, p. 161.

Clement M., Iborra E., Sangrador J., Sanz-Hervás, A., Vergara, L. and Aguilar, M., 2003. "Influence of sputtering mechanisms on the preferred orientation of aluminum nitride films". *Journal of Applied Physics*, Vol. 94 (3), p.1495.

Ferreira, F., Sousa, C., Cavaleiro, A., Anders, A. and Oliveira, J., 2017. "Phase tailoring of tantalum thin films deposited in deep oscillation magnetron sputtering mode". *Surface and Coatings Technology*, Vol. 314, p. 97.

García-Farrera, B., Murillo, A. E., Melo-Máximo, D.V., Salas, O., Melo-Máximo and L., Oseguera, J., 2017. "Effect of the Electrode Layer on the Deposition of AlN for Biosensors". Journal of Bio-Tribocorrosion, Vol. 3, p.15.

Gudmunson, J.T., Brenning, N., Lundin, D. and Helmersson, U., 2012. "High power impulse magnetron sputtering discharge". *Journal of Vacuum Science and Technology A*, Vol. 30(3), p. 030801.

Iqbal, A., Walker, G., Iacopi, A. and Mohd-Yasin, F., 2016. "Controlled Sputtering of AlN (002) and (101) crystal orientations on epitaxial 3C-SiC-on-Si (100) substrate". *Journal of Crystal Growth*, Vol. 440, p. 76.

Lin, J., Wang, B., Sproul, W.D., Ou, Y. and Dahan, I., 2013. "Anatase and rutile TiO_2 films deposited by arc-free deep oscillation magnetron sputtering". *Journal of Physics D: Applied Physics*, Vol. 46, p. 084008.

Lin, J. and Chistyakov, R., 2017. "C-axis orientated AlN films deposited using deep oscillation magnetron sputtering". *Applied Surface Science*, Vol. 396, p. 129.

Oliveira, J.C., Fernandes, F., Ferreira, F. and Cavaleiro, A., 2015. "Tailoring the nanostructure of Ti-Si-N thin films by HIPIMS in Deep oscillation magnetron sputtering (DOMS) mode". *Surface and Coatings Technology*, Vol. 264, p. 140.

Yang, Y-C., Chang, C-T., Hsiao, Y-C., Lee, J-W. and Lou, B-S., 2014. "Influence of high power impulse magnetron sputtering pulse parameters on the properties of aluminum nitride coatings". *Surface and Coatings Technology*, Vol. 259, p. 219.

TET, http://www.engineeringtoolbox.com/linear-expansion-coefficients-d_95.html

7. RESPONSIBILITY NOTICE

The authors (are) the only responsible for the printed material included in this paper.